Evolution of the nitric oxide synthase family in vertebrates and novel insights in gill development

Giovanni Annona[1], Iori Sato[2], Juan Pascual-Anaya[3,†], David Osca[4], Ingo Braasch[5], Randal Voss[6], Jan Stundl[7,8,9], Vladimir Soukup[7], Shigeru Kuratani[2,3], John H. Postlethwait[10], Salvatore D'Aniello[1,*]

[1] Biology and Evolution of Marine Organisms, Stazione Zoologica Anton Dohrn, 80121, Napoli, Italy

[2] Laboratory for Evolutionary Morphology, RIKEN Center for Biosystems Dynamics Research (BDR), Kobe, 650-0047, Japan

[3] Evolutionary Morphology Laboratory, RIKEN Cluster for Pioneering Research (CPR), 2-2-3 Minatojima-minami, Chuo-ku, Kobe, Hyogo, 650-0047, Japan

[4] University Institute of Environmental Studies and Natural Resources (IUNAT). Faculty of Marine Sciences. University of Las Palmas de Gran Canaria. Canary Islands, Spain

[5] Department of Integrative Biology and Program in Ecology, Evolution & Behavior (EEB), Michigan State University, East Lansing, MI 48824, USA

[6] Department of Neuroscience, Spinal Cord and Brain Injury Research Center, and Ambystoma Genetic Stock Center, University of Kentucky, Lexington, Kentucky, USA

[7] Department of Zoology, Faculty of Science, Charles University in Prague, Prague, Czech Republic

[8] Division of Biology and Biological Engineering, California Institute of Technology, Pasadena, CA, USA

[9] South Bohemian Research Center of Aquaculture and Biodiversity of Hydrocenoses, Faculty of Fisheries and Protection of Waters, University of South Bohemia in Ceske Budejovice, Vodnany, Czech Republic

[10] Institute of Neuroscience, University of Oregon, Eugene, OR 97403, USA

[†] Present address: Department of Animal Biology, Faculty of Sciences, University of Málaga; and Andalusian Centre for Nanomedicine and Biotechnology (BIONAND), Málaga, Spain

* Correspondence: salvatore.daniello@szn.it

Abstract

Nitric oxide (NO) is an ancestral key signaling molecule essential for life and has enormous versatility in biological systems, including cardiovascular homeostasis, neurotransmission and immunity. Although our knowledge of nitric oxide synthases (Nos), the enzymes that synthesize NO *in vivo*, is substantial, the origin of a large and diversified repertoire of *nos* gene orthologs in fish with respect to tetrapods remains a puzzle. The recent identification of *nos3* in the ray-finned fish spotted gar, which was considered lost in this lineage, changed this perspective. This finding prompted us to explore *nos* gene evolution and expression in depth, surveying vertebrate species representing key evolutionary nodes. This study provides noteworthy findings: first, *nos2* experienced several lineage-specific gene duplications and losses. Second, *nos3* was found to be lost independently in two different teleost lineages, Elopomorpha and Clupeocephala. Third, the expression of at least one *nos* paralog in the gills of developing shark, bichir, sturgeon, and gar but not in arctic lamprey suggests that *nos* expression in this organ may have arisen in the last common ancestor of gnathostomes. These results provide a framework for continuing research on *nos* genes' roles, highlighting subfunctionalization and reciprocal loss of function that occurred in different lineages during vertebrate genome duplications.

Keywords: Vertebrate evolution; Genome duplication; Gene duplication and loss; NOS; Phylogenomics; Synteny.

Introduction

Historically classified as a pollutant, nitric oxide (NO) was recognized as “Molecule of the Year" in 1992 [1] for its important function as a cellular signaling molecule. NO plays a role in a myriad of physiological processes, including cardiovascular homeostasis [2], neurotransmission [3], immune response [4], and in neurodegenerative diseases [5] and cancer [6].

Nitric oxide synthase (Nos), the enzyme catalysing the biosynthesis of NO *in vivo*, is ubiquitous among organisms [7,8]. Three *nos* gene paralogs have been described in vertebrates: two constitutively expressed genes, including *nos1* (also known as *neuronal nos*, or *nNos*), which represents the predominant source of NO involved in neurogenesis and neurotransmission [9,10], and *nos3* (*endothelial nos* or *eNos*) implicated in angiogenesis and blood pressure control in vascular endothelial cells [11,12]. In addition, *nos2* (*inducible nos* or *iNos*), whose expression is instead evoked by proinflammatory cytokines, is promptly activated in a range of acute stress responses [13].

Although the availability of current genomic data covers all major ray-finned fish lineages, the evolutionary history of their *nos* gene repertoire remains puzzling. Previous studies reported a variable number of *nos* genes in teleost fishes: *nos1* is always present in a single copy; *nos2* either in one or two copies, probably due to the additional teleost-specific whole-genome duplication (TGD) [14–17], or absent as observed in several species. On the other hand, *nos3* has been reported as missing in the genomes of ray-finned fish. This apparent gene loss contrasts with literature describing a putative Nos3-like protein localized by antibody stains in gills and vascular endothelium of several teleost species [18,19]. The discovery of a *nos3* ortholog in the spotted gar *Lepisosteus oculatus,* a holostean fish (the sister group of teleosts within the ray-finned lineage) [20], and the variable number of teleost *nos2* genes raises new questions about the evolution of this

84 important gene family, including: *i*. is our current view on the origin and evolution of *nos*
85 gene family in vertebrates accurate?; and *ii*. can further investigation of *nos* expression
86 pattern in fish retaining a *nos3* copy reveal novel functional insights? In an attempt to
87 answer these questions, we have studied the Nos family repertoire at unprecented
88 phylogenetic resolution, investigated conserved syntenies in fish genomes, and studied
89 the expression pattern of all three *nos* genes during development in multiple species
90 representing key nodes in vertebrate evolution.
91

92 ## Results

93 **Revised evolutionary history of Nos2 and Nos3**

94 Gaps in our current knowledge of Nos family evolution include the time of origin of the
95 three distinct paralogous *nos* genes and when some of them were secondarily lost in
96 specific lineages. We reconstructed the Nos phylogeny using 108 protein sequences from
97 53 species (electronic supplementary material, Table S1) providing a broad representation
98 of aquatic vertebrates: cyclostomes (modern jawless fish), chondrichthyans (cartilaginous
99 fish), and osteichthyes (bony fish) including ray- and lobe-finned fishes. Lobe-finned fishes
100 include coelacanths, lungfishes, and tetrapods; Ray-finned fishes comprise the non-teleost
101 lineages of polypteriformes (e.g. bichir), acipenseriformes (e.g. sterlet sturgeon),
102 holosteans (lepisosteiformes, e.g. spotted gar, and amiiformes, e.g. bowfin), and the
103 teleosts, subdivided into three major living lineages: elopomorphs (e.g. eels and relatives),
104 osteoglossomorphs (e.g. arowana, mooneyes, and the freshwater elephantfish), and
105 clupeocephalans (e.g. zebrafish and medaka) [21] (for clarification see electronic
106 supplementary material, figure S1).
107 All Nos proteins considered in the present study showed conservation of canonical
108 domains organization. Our phylogenetic analysis confirmed the presence of Nos1 in all

jawed vertebrates examined (figure 1a, green shading). In contrast, most fish lineages retained Nos2, including chondrichthyans (*Callorhinchus milii, Rhincodon typus, Chiloscyllium punctatum,* and *Scyliorhinus torazame*), polypteriformes (*Polypterus senegalus*, *Erpetoichthys calabaricus*), acipenseriformes (*Acipenser ruthenus*), holosteans (*Amia calva, Lepisosteus oculatus*), elopomorphs (*Megalops cyprinoides*), osteoglossomorphs (*Paramormyrops kingsleyae, Scleropages formosus*) and coelacanthiformes (*Latimeria chalumnae*) (figure 1a, grey shading), although a *nos2* gene loss event occurred at the stem of Neoteleostei (figure 1b), since it has not been found in any available genomic or transcriptomic data from this clade. On the other hand, our phylogenetic analysis highlights the occurrence of extra *nos2* duplicates in several lineages, for which we adopted a specific nomenclature based on the phylogenetic analysis and synteny conservation: in the zebrafish *Danio rerio* there are two *nos2* genes, *nos2a* and *nos2b*, while in the goldfish *Carassius auratus*, the blind golden-line barbel *Sinocyclocheilus anshuiensis* and the common carp *Cyprinus carpio* we found three: *nos2a*, *nos2ba,* and *nos2bb*; in salmonids (*Salmo salar* and *Oncorhynchus mykiss*) there are two different copies of *nos2*, named *nos2α* and *nos2β*; and lastly, the two *nos2* paralogs that we found in a characid (the Mexican tetra *Astyanax mexicanus*), a gymnotid (the electric eel *Electrophorus electricus*), an ictalurid (the channel catfish *Ictalurus punctatus*), an esocid (the northern pike *Esox lucius*), and a clupeid (the Atlantic herring *Clupea harengus*) were named *nos2.1* and *nos2.2* (figure 1a, grey shading).

Nos3 deserves special attention since it was previously believed that a loss event predated the lineage of actinopterygians or alternatively that it represents an innovation of tetrapods [8]. Nevertheless, this hypothesis may have been overinterpreted since few ray-finned genome sequences were originally available. The only actinopterygian *nos3* gene reported thus far was in the spotted gar [20]. Here we report the identification of *nos3*

genes in genomes of the bichir *P. senegalus*, the sterlet sturgeon *A. ruthenus* [22], the bowfin *A. calva* [23], and the freshwater elephantfish *P. kingsleyae* [24] (figure 1a, red shading). The absence of *nos3* in clupeocephalans indicates a gene loss event in the stem of this group (figure 1c). Furthermore, we did not find *nos3* in the tarpon *M. cyprinoides*, the most complete genome available among Elopomorpha, nor in transcriptomic data of the European eel *Anguilla anguilla*. On the other hand, we did identify a *nos3* ortholog in the cloudy catshark *S. torazame,* suggesting its presence in the ancestor of gnathostomes. Previously, two *nos* genes had been found in the lamprey, called *nosA* and *nosB* [8], with unresolved orthology to gnathostome *nos1-nos2-nos3*, and derived from a lineage-specific tandem duplication in the lamprey lineage. Based on this finding, we searched for the presence of *nos* genes in other cyclostomes. We found orthologous genes to *P. marinus nosA* and *nosB* paralogs in the arctic lamprey *Lethenteron camtschaticum* [25], and a single *nos* gene in the inshore hagfish *Eptatretus burgeri*. Our phylogenetic analysis shows that the hagfish Nos remains outside lamprey NosA-NosB clade, therefore with no clear orthology relationship to any specific gnathostome Nos1, Nos2, Nos3, and suggesting that the duplication giving rise to the lamprey *nosA-nosB* occurred at least before the last common ancestor of Petromyzontidae.

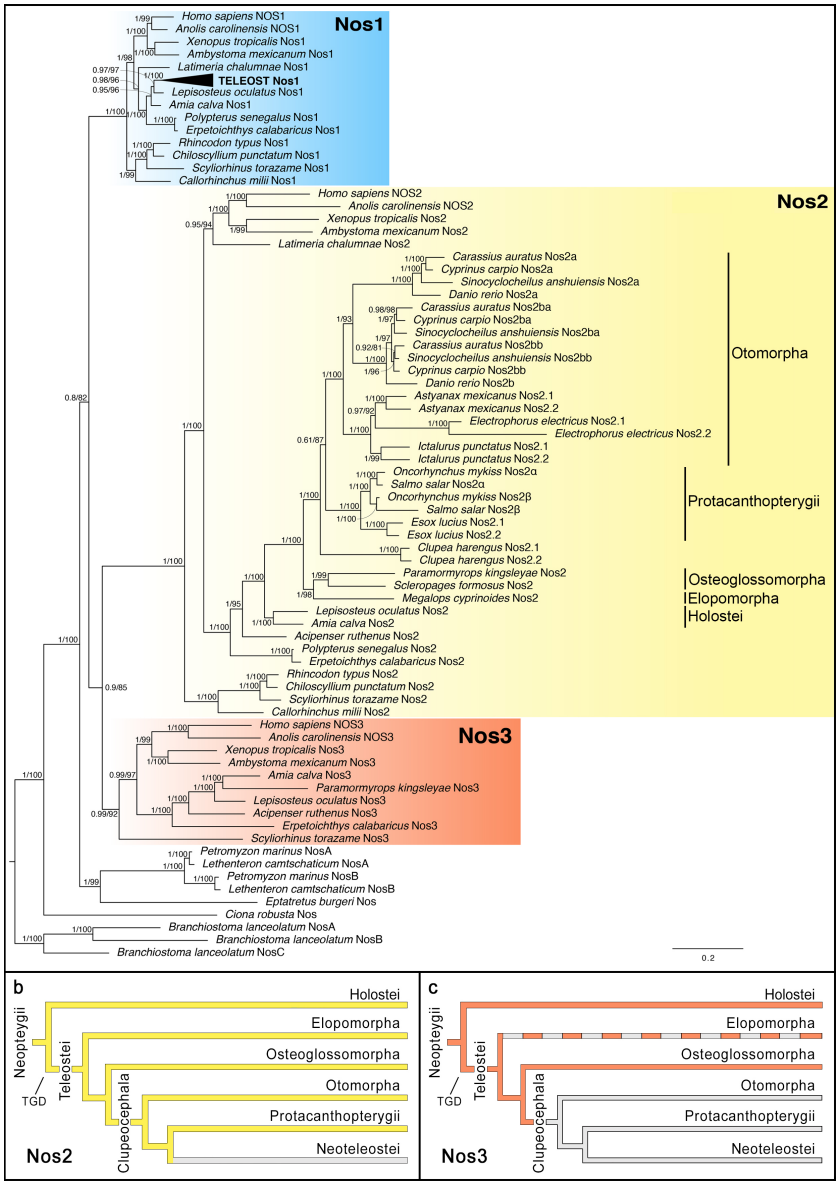

Figure 1. Evolution of the Nos gene family. a) Phylogenetic analysis of Nos proteins in chordates. The tree topology was inferred by Bayesian inference and maximum-likelihood methods, with the exact topology obtained from the former shown here (see electronic supplementary material, figure S2 for the maximum-likelihood tree). Numbers at nodes represent posterior probability values (left) and maximum-likelihood bootstrap support for

1000 replicates (right). The cyan-blue box highlights the Nos1 clade, the yellow box the Nos2 clade and a red-orange box the Nos3 clade. **b-c)**, Evolutionary scenarios indicating the loss of Nos2 event in Neoteleostei (**b**) and Nos3 in Clupeocephala (**c**) as grey lines. Nos3 in Elopomorpha is absent although parsimony suggests it was present in stem elopomorphs, and it is indicated with a dashed line. TGD stands for Teleost-specific Genome Duplication.

In order to study the Nos evolution at the protein level and verify if each gene clade is under differential selection pressure we conducted a Branch Model (BM) analysis. The BM analysis showed significant p-value and lower ω values for Nos1 (ω1=0.043) and Nos2 (ω1=0.124) compared to the rest of the clades (electronic supplementary material, Table S2). Therefore they seem to be under purifying (negative) selection, and in particular the Nos2 evolution resulted slightly more relaxed in respect to the rest of the genes analysed. In the case of Nos3 the BM analysis showed a not significant p-value therefore no evidence of positive selection was found in comparison to the other two paralogues (electronic supplementary material, Table S2).

In order to better understand the gene loss and expansion events highlighted by our phylogenetic analysis, we next analysed the microsynteny (genes linked in proximity) of *nos* genes in different species. This revealed a complex evolutionary scenario for *nos2* compared to *nos1* and *nos3*. Specific *nos2* duplications in different lineages are explained by distinct evolutionary events in teleosts (figure 2a and electronic supplementary material, figure S3). First, the lack of synteny conservation between *nos2a* and *nos2b* in cyprinids, and the lack of *nos2a* in the expected location in non-cyprinid fishes (electronic supplementary material, figure S3) indicates that these paralogs originated in a specific gene duplication event in a common ancestor of the lineage, independently from the TGD (the alternative explanation would require numerous *nos2a* losses in several fish lineages), in which while *nos2b* has remained in the ancestral genomic location, *nos2a* has been translocated to a different position in the genome (figure 2a and electronic supplementary

material, figure S3). Second, an additional genome duplication event after the TGD specifically occurred independently in several teleost lineages, causing the presence of extra *nos2* paralogs. These include some cyprinids, in which a carp-specific genome duplication event (Cs4R) likely occurred before the divergence of *C. auratus*, *S. anshuiensis* and *C. carpio* [26], and salmonids (salmonid-specific genome duplication or Ss4R) [27,28], with *S. salar* and *O. mykiss* in this study. These additional tetraploidization events can explain the origin of the two independent sets of *nos2* genes in cyprinid and salmonid species. In the case of cyprinids, both our phylogenetic and synteny analyses clearly show their *nos2b* orthology, and we denote them as *nos2ba* and *nos2bb* (figure 1a and figure 2a). In the case of salmonids, we name them *nos2α* and *nos2β* to distinguish them from the cyprinid *nos2a* and *nos2b* paralogs, which have a separate origin (see above; figure 2a). Third, independent tandem gene duplications explain the presence of two nos2 copies, that we named *nos2.1* and *nos2.2*, located next to each other in the same chromosomal fragment in the genomes of the Atlantic herring (*C. harengus*), the Mexican tetra (cavefish, *A. mexicanus*), the electric eel (*E. electricus*), the channel catfish (*I. punctatus*), and the northern pike (*E. lucius*) (figure 2a).

Bichir, reedfish, sterlet, spotted gar, bowfin and freshwater elephantfish are the only ray-finned fishes that retained a *nos3* ortholog. Therefore, we investigated the absence of *nos3* in clupeocephalans. First, we looked for the genomic region containing *nos3* in fishes that represent outgroups to the clupeocephalans. We found one long scaffold of the *P. kingsleyae* genome (scaffold 217) [24] showing extensive conserved synteny with the *nos3*-containing segment of the linkage group 11 (LG) in the spotted gar genome (figure 2b). While these appear to correspond to one of the TGD ohnologons (figure 2b), there are other two *P. kingsleyae* scaffold segments (from scaffolds 72 and 104) that together seem to represent the second TGD ohnologon, but lacking the expected *nos3* TGD ohnolog

211 (figure 2b). Zebrafish chromosomes 16 and 19 and medaka chromosomes 11 and 16
212 contain orthologous regions to the two *P. kingsleyae* and *L. oculatus* TGD ohnologons, but
213 lack a *nos3* gene at the expected locations. One-to-one relationship between these *P.*
214 *kingsleyae* scaffolds and zebrafish and medaka chromosomes is challenging to determine
215 (figure 2b). Regardless, the most parsimonious explanation for the nos3 repertoire in ray-
216 finned fishes is that, one of the two *nos3* TGD ohnologs was lost in the teleost common
217 ancestor, while the other was retained and later lost in secondary, independent events in
218 the common ancestor of Clupeocephala and, probably, that of Elopomorpha (figure 1c and
219 figure 2b).

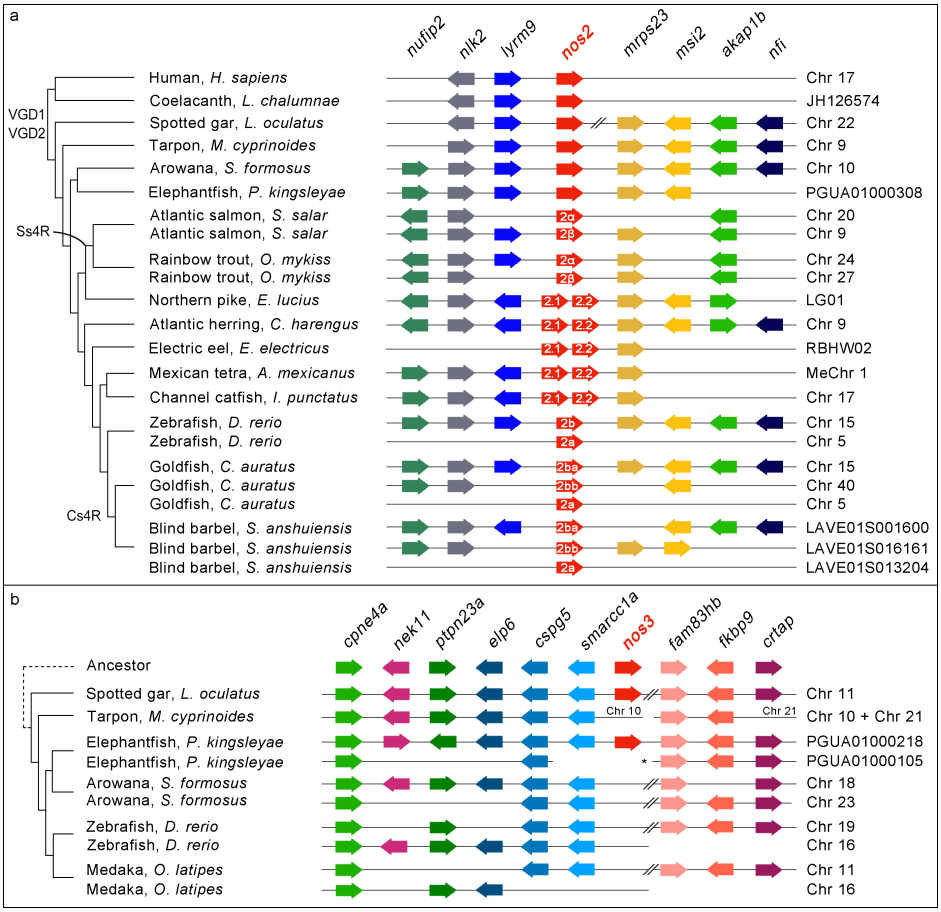

Figure 2. Conserved microsynteny of *nos2* and *nos3*. **a**, The *nos2* paralogs derived from different duplication modalities: carp-specific genome duplication (Cs4R) (*nos2ba* and *nos2bb* in the goldfish and blind golden-line barbel); salmonid-specific genome duplication (Ss4R) (*nos2α* and *nos2β* in the Atlantic salmon and rainbow trout); tandem gene duplication occurred independently in five lineages (*nos2.1* and *nos2.2* in the northern pike, Atlantic herring, electric eel, Mexican tetra and channel catfish). An additional *nos2* duplicate (*nos2a*) is present in cyprinids (zebrafish, goldfish, and blind barbel) (see electronic supplementary material, figure S3). **b**, A conserved synteny map of genomic regions around the *nos3* gene locus highlights the loss in Clupeocephala (including zebrafish and medaka), and in Osteoglossomorpha (arowana). Consecutive genes are represented as arrows and are colour coded according to their orthology and ohnology. The direction of arrows indicates gene transcription orientation. The symbol // indicates long-distance on the chromosome (>600 kb). The asterisk indicates scaffold 72 of the freshwater elephantfish genome [24].

Expression of *nos* in vertebrate developing gills

Spotted gar is an important emerging model organism representing an evolutionary bridge between teleosts and tetrapods that facilitates cross-species comparisons. The gar genome is slowly evolving compared to that of teleosts and has preserved a more ancient structural organization [29]. Therefore, we examined the expression patterns of *nos* genes during gar development. As expected, based from the literature, *nos1* was expressed in several regions of the developing nervous system (electronic supplementary material, figure S4). In contrast, *nos2* expression was not detected during the developmental stages covered in the present study, i.e., from 4 to 14 days post fertilization (dpf). Unexpectedly, the expression of *nos3* was first detected in embryos in the pharyngeal area at 4 dpf (figure 3a-b) and increased at 6 dpf (figure 3c-d). At 7 dpf, embryos showed clear *nos3* expression in developing arches III, IV, and V (figure 3e-g). Later, at 11 dpf, the positive signal is localized in gill filaments (figure. 3i-k). Histological sections highlighted the presence of *nos3* in the epithelium of branchial lamellae (figure 3l), also confirmed by the signal in gill structures in an advanced stage of maturation in 14 dpf juveniles (figure 3m-p).

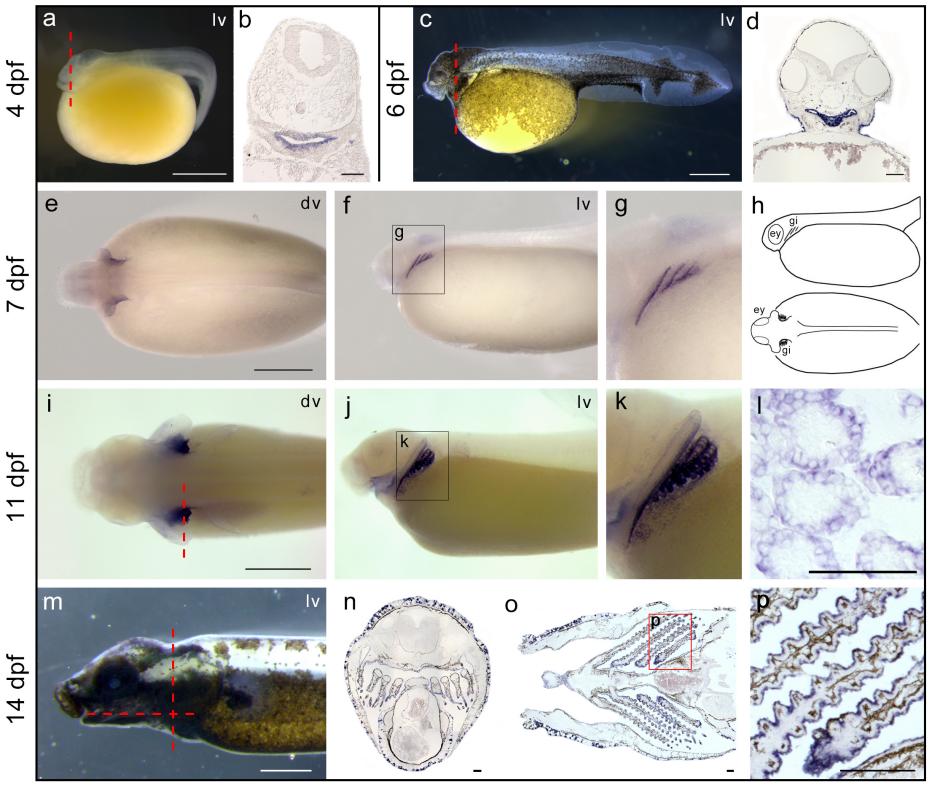

Figure 3. Spotted gar *nos3* localization during development. Expression of *nos3* is localized in the pharyngeal area in 4 dpf (**a-b**) and 6 dpf (**c-d**) embryos, in pharyngeal arches in 7 dpf larvae (**e-g**) schematized in (**h**), in developing gills in 11 dpf late larvae (**i-l**), and in gill lamellae in 14 dpf juveniles (**m-p**). Coronal (**n**) and transversal section (**o**) planes are indicated with a red dashed line in (**m**). Abbreviations: ey, eye; gi, gill; dv, dorsal view; lv, lateral view. Scale bar is 1 mm in a, c, e, i, m; 100 µm in b, d, l, n, o, p.

The detection of *nos3* transcripts in gills of spotted gar and the established involvement of NO gas in osmoregulatory control and vascular motility in gills of numerous teleosts [30–35] prompted us to investigate whether a similar *nos* expression patterns occurred in developing gills of other fish species. We investigated *nos* expression in the sterlet sturgeon *A. ruthenus* and the bichir *P. senegalus,* members of early-branching groups of

ray-finned fishes [21]. Moreover, we similarly investigated *nos* expression in the chondrichthyan cloudy catshark *S. torazame* to infer the ancestral expression condition among gnathostomes. Unlike gar, we discovered that *nos3* was not expressed in gills of other species analysed in this work (electronic supplementary material, figure S4), thus raising questions of whether *nos3* expression in gills represents an oddity of holosteans or gars. Surprisingly, we found a different scenario in which other nos genes were expressed in gills of sturgeon, bichir, and shark. In particular, *nos2* was expressed in the branchial area of the sterlet sturgeon (figure 4a-c) and bichir embryos (figure 4d-f), while *nos1* is expressed in gills of catshark embryos (figure 4g-i).

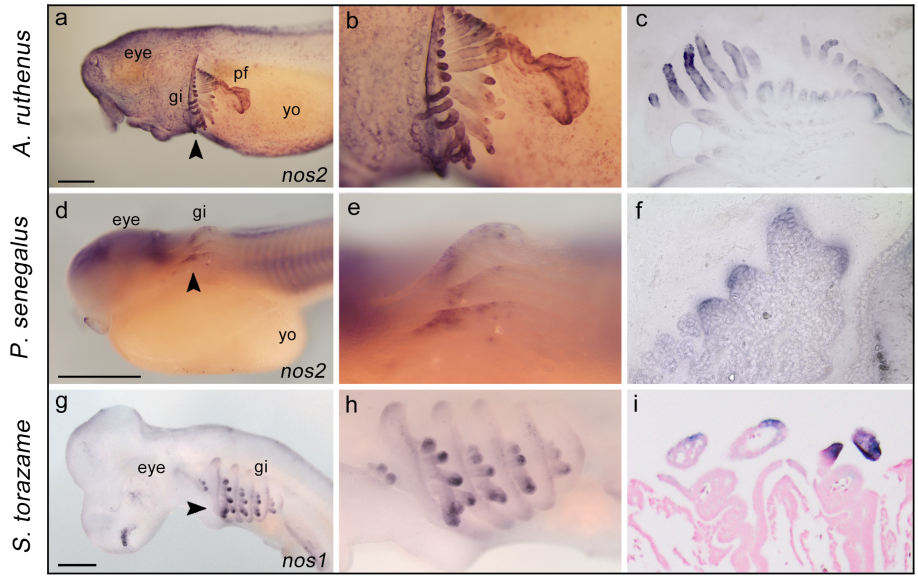

Figure 4. Expression of *nos* genes in developing gills of sturgeon, bichir, and shark embryos. The expression of *nos2* in the gills of sterlet sturgeon *Acipenser ruthenus* (14 mm stage, **a-c**) and bichir *Polypterus senegalus* (stage 31, **d-e**); *nos1* in the shark *Scyliorhinus torazame* (stage 27, **g-i**). Higher magnification views of the gill structure of **a, d, g** are shown in **b, e**, **h**, respectively. The arrowheads indicate sectioning plane (**a, d, g**): transversal sections (**c, f**, 50 µm) and frontal section (**l**, 10 µm). Abbreviations: gi, gill; yo, yolk; pf, pectoral fin. Scale bar in a, d, g is 0.5 mm.

285

286 Our results show that *nos* paralogs are expressed in pharyngeal arches and gills in both
287 actinopterygians and chondrichthyans. These findings lead us to question whether *nos*
288 expression in gills could be a conserved feature also in sarcopterygians, and in particular
289 in amphibians that use gills for gas exchange. Therefore, to investigate the presence of
290 *nos* transcripts in amphibia, we chose the neotenic axolotl *Ambystoma mexicanum*
291 because it retains functional external gills throughout life. Gene expression analysis by
292 qPCR revealed that *nos1* and *nos2* are almost not detectable in adult axolotl gills, while
293 *nos3* turned out to be highly expressed in gill structures (electronic supplementary
294 material, figure S5). Therefore, we conclude that *nos* expression in gills is a conserved
295 feature in neotenic amphibian assayed, previously observed exclusively in fishes.

296

297 **Expression of *nos* genes in the lamprey**

298 In cyclostomes (jawless vertebrates, including lampreys and hagfish), cartilaginous and
299 bony gnathostomes (jawed vertebrates), gills are endoderm-derived structures, pointing to
300 a single origin of pharyngeal gills before the divergence of these vertebrate lineages
301 [36,37]. To assess whether *nosA* and *nosB* are expressed in gills during embryogenesis,
302 we performed whole-mount *in situ* hybridization experiments at different embryonic stages.
303 We found that lamprey *nosA* was expressed in several tissues, including the brain, dorsal
304 midline epidermis, tailbud, mouth, and cloaca, but not in gills (figure 5a-b). Conversely, the
305 lamprey *nosB* paralog showed restricted expression in the developing mouth, specifically
306 in the cheek process, including upper and lower lip regions (figure 5c-d). These results
307 show that in the arctic lamprey, neither of the two *nos* paralogs is expressed in immature
308 or mature gills, suggesting a fundamental difference in the role of *nos* genes in jawless
309 and jawed vertebrates.

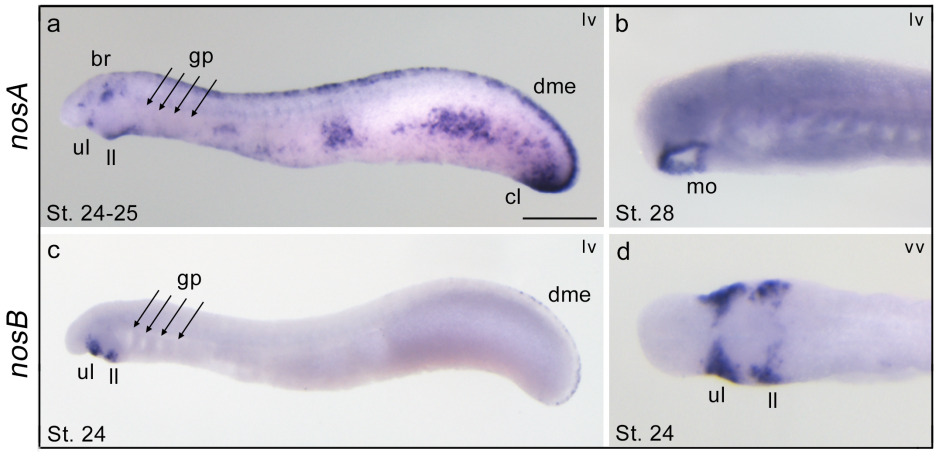

Figure 5. Expression patterns of *nosA* and *nosB* in larvae of the arctic lamprey. At stage 24-25 the *nosA* is expressed in the brain, mouth, upper and lower lip, dorsal midline epidermis, and cloaca (**a**). At stage 28, *nosA* expression is restricted to the mouth (**b**). The *nosB* is exclusively expressed in the cheek process, consisting of upper and lower lips (**c-d**), and faint expression in the dorsal midline epidermis (**c**). Abbreviations: br, brain; cl, cloaca; dme, dorsal midline epidermis; gp, gill pouches; mo, mouth; ll, lower lip; ul, upper lip; lv, lateral view; vv, ventral view. Scale bar in a is 0.5 mm.

Discussion

Actinopterygian fishes experienced one of the largest radiations in the animal kingdom and their history represents a valuable resource for the formulation of hypotheses regarding the evolution of vertebrate gene families. In this work, we employed data from recent genome projects to clarify and update the evolution of Nos family across vertebrates. We performed a phylogenetic reconstruction using Nos protein sequences from key vertebrate groups, including cyclostomes for which little information has previously been available. Our phylogenetic analysis confirmed that Nos1 is ubiquitously present as single copy gene across the gnathostome lineage, at least in the covered osteichthyan and chondrichthyan species. Branch lengths of the Nos1 clade suggest a slow evolutionary rate throughout

vertebrate evolution in respect to the other two *nos* genes. Furthermore, our phylogenetic data, complemented with syntenic analyses, highlighted for the first time a highly complex scenario of Nos2 evolution, for which we suggest a nomenclature that attempts to incorporate evolutionary origins into gene names. Previous analyses showed the presence of two *nos2* genes (*nos2a* and *nos2b*) in zebrafish and goldfish [38,39], likely originated from an event of gene duplication that occurred specifically at the stem of the group, and not related to the classic TGD. This result is supported by synteny analysis since the chromosomal position of *nos2a* and *nos2b* genes is not conserved (figure 2a and electronic supplementary material, figure S3), as it would be expected if they were retained after a whole-genome duplication. Here we show the presence of a *nos2a* paralog also in other two cyprinids, *C. carpio* and *S. anshuiensis* (figure 1a and figure 2a). On the other hand, the cyprinid *nos2b* paralog independently duplicated in carps after the Cs4R [26], as the conserved synteny suggests (figure 2a). In salmonids, synteny analysis also implies that the two Nos2 paralogs originated secondarily after the Ss4R (figure 2a) [27,28]. Here, we call these genes *nos2ba* and *nos2bb* in carps to emphasize and clarify their relationships to zebrafish genes, and *nos2α* and *nos2β* in salmonids to indicate their distinct evolutionary origin. Additionally, the present work shows that *nos2* has undergone several independent lineage-specific tandem gene duplication events (*nos2.1* and *nos2.2*) (figure 2a). The search of *nos2* in available fish genomes, covering all main groups, failed to find it in any Neoteleostei, and for this reason, we hypothesized a *nos2* gene loss event occurred in stem Neoteleostei (figure 1 and figure 6). It is worth mentioning that NO produced upon stimulation of the inducible *nos* (*nos2*) is considered one of the most versatile players of the immune system against infectious diseases, autoimmune processes and chronic degenerative diseases [4,40]. For this reason, it would be important in the future to investigate the impact of Nos2 loss on the immune response in

Neoteleostei and if any compensatory mechanisms occurred through the activation of other *nos* paralogs. In addition, Nos2 is the only *nos* gene with retained duplicates in vertebrates, therefore, it would also be important to understand if *nos2* duplicates underwent neofunctionalization or subfunctionalization, thus providing new functional features to the organism.

Concerning *nos3*, our understanding of its evolutionary history had a twist with the finding of a *nos3* ortholog in the spotted gar genome [20], proving that the previously postulated actinopterygian-specific loss of *nos3* was an incorrect inference. Fostered by this discovery, we specifically searched for the presence of *nos3* orthologs in a wide range of fish species to infer the ancestral condition. We identified a *nos3* gene in bowfin, thus confirming the presence of *nos3* in the other reference genus of the holostean clade, in addition to gar (figure 1a and figure 6). Furthermore, the presence of *nos3* in genomes of bichir and sterlet sturgeon, which diverged prior to the teleostean and holostean split, confirmed the hypothesis that *nos3* was already present in the common ancestor of extant osteichthyans, rather than an innovation of tetrapods [8] or neopterygians (holosteans plus teleosts) [20] (figure 6). We did not find *nos3* gene in the tarpon *M. cyprinoides* genome (figure 2b), and to date, the limited genomic and transcriptomic data of eels, congers, and morays cannot endorse the presence of a *nos3* in Elopomorpha. Therefore, more genome sequences are necessary to confirm its absence in this key group. We also did not find *nos3* in any fish from Clupeocephala (non-elopomorph and non-osteoglossomorph teleosts; figure 1a and figure 2b) suggesting that a loss event took place in the common ancestor of clupeocephalans (figure 1c and figure 2b). Notably, we found a *nos3* gene in the osteoglossomorph elephantfish *P. kingsleyae* (figure 1a and figure 2b), and it allowed us to confirm that the loss of *nos3* did not occur in the last common teleost ancestor, as previously thought [20]. These findings suggest instead the following evolutionary scenario

for the *nos3* gene: first, since we only find a maximum of one *nos3* gene in those cases where it is present, we assume that one of the two TGD ohnologs was immediately lost after the TGD, and the other one was retained. This *nos3* gene was then lost in the ancestors of elopomorphs –although further research is needed to confirm this– and clupeocephalans independently in separate events (figure 6).

The discovery of *nos3* in sharks (*S. torazame* in this study) suggests that the origin of *nos3* predates the divergence of gnathostomes and that three distinct *nos* paralogs were already present in the last common ancestor of gnathostomes (figure 6), likely originating after the two rounds of whole-genome duplication that took place during early vertebrate evolution (VGD1 and VGD2, 2R hypothesis) [8] [41] [Nakatani et al., 2021). The origin of *nos* genes is, in fact, supported by the linkage to the evolutionarily conserved *Hox* gene clusters and several other syntenic genes (figure 6b and electronic supplementary material, figure S6). Under this scenario, then a fourth *nos* gene (putative *nos4*) should have existed but was apparently lost early in the gnathostome evolution (figure 6a).

The apparent lack of *nos*3 in some vertebrate lineages, such as in coelacanth *L. chalumnae* (an extant basally diverging sarcopterygian), in arowana *S. formosus* (an osteoglossomorph), and in elopomorph fishes, remains to be clarified. In the future, further genomic projects will surely fill these gaps in our understanding of this fascinating gene family.

Commented [SD1]: Nakatani, Y., Shingate, P., Ravi, V. *et al.* Reconstruction of proto-vertebrate, proto-cyclostome and proto-gnathostome genomes provides new insights into early vertebrate evolution. *Nat Commun* **12,** 4489 (2021). https://doi.org/10.1038/s41467-021-24573-z

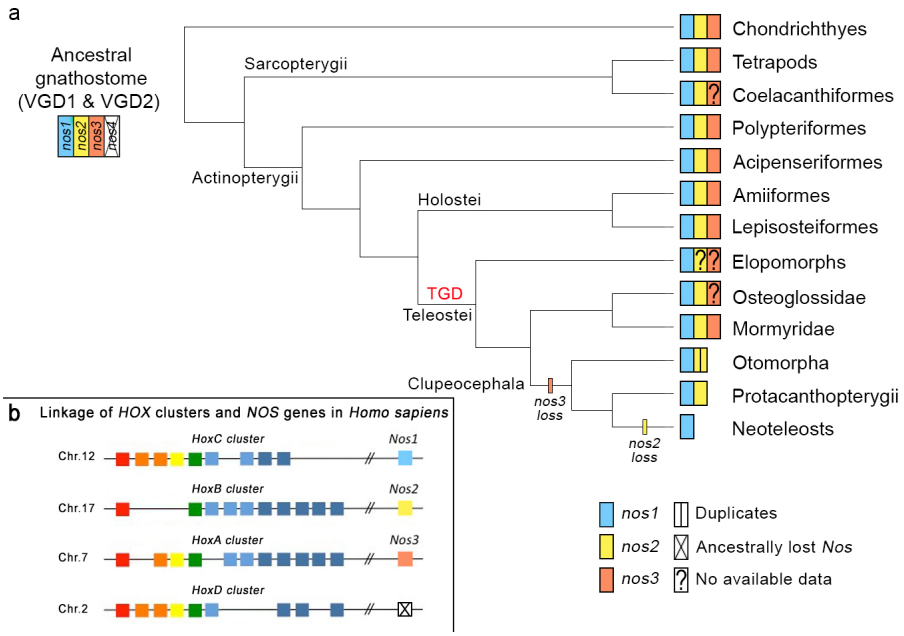

Figure 6. *Nos* evolution in light of recent gene findings in vertebrates. The proposed evolution of *nos* genes in gnathostomes (**a**) supposes an ancestral loss of a predicted fourth *nos* gene (grey box), based on the linkage of human *nos* and *Hox* clusters (**b**). Loss of *nos3* occurred in stem Clupeocephala and loss of *nos2* in stem Neoteleostei (**a**). Species-specific *nos2* duplications occurred in some Otomorpha, including Cyprinidae and Characidae families.

The protein evolution analysis highlighted that the three Nos clades show a different selection pressure as Nos1 is under strong negative selection, Nos2 under relaxed negative selection and, being largely lost in almost all teleost, Nos3 is probably under positive selection although we could not calculate a significant ω value for this gene clade. These results are in accordance with the Nos family evolutionary history, being Nos1 always present in all species analysed so far, Nos2 lost or duplicated in several lineages, and Nos3 massively lost during fish evolution.

417 The importance of NO in the ontogeny and function of vertebrate gills has already been
418 documented in the context of physio-pharmacological studies, primarily using inhibitors of
419 Nos activity. In gills, NO acts as a paracrine and endocrine vasoactive modulator and,
420 therefore, plays a crucial role in the distribution of oxygenated blood [42]. Moreover, NO
421 has an osmoregulatory function controlling the movement of ions across the gill epithelium
422 [33,43–45], and represents an important molecular component of the immune system
423 employed by macrophages to attack and destroy pathogens [46]. Nevertheless,
424 documentation of Nos enzymatic activity in fish gills has relied exclusively upon techniques
425 unable to discriminate among individual Nos proteins, such as NADPH-diaphorase activity
426 and immunolocalization with heterologous mammalian antibodies [42,44,45,47]. Therefore,
427 the detected enzymatic activity has for a long time been indicated generically as 'Nos-like'.
428 Here we used a different approach based on mRNA transcript detection methodology,
429 which unequivocally distinguishes different genes, and showed, for the first time, that
430 indeed *nos* genes are expressed in gills during development in various vertebrates.
431 Surprisingly different Nos paralogs are expressed in gills in different animals tested: *nos1*
432 in shark, *nos2* in bichir and sterlet sturgeon, and *nos3* in spotted gar. The most
433 parsimonious hypothesis to explain this result is that the ancestral *nos* gene had a number
434 of roles in gills, immune system, brain, and other organs that was controlled by separate
435 regulatory elements and, due to subfunctionalization after the vertebrate 2R (according to
436 the Duplication-Degeneration-Complementation (DDC) model) [48], these physiological
437 roles partitioned to different *nos* ohnologs as lineages diverged and reciprocal loss of the
438 gill expression function occurred in a lineage-specific way. Further support to this
439 hypothesis comes from the identification of *nos1*-positive cells in gill of zebrafish at 5 dpf,
440 in addition to brain, eye, periderm and NaK ionocytes, according to the recently released

441 developmental single-cell transcriptome atlas [49] (electronic supplementary material,
442 figure S7).
443 Additionally, to corroborate the involvement of NO in normal gill physiology, we searched
444 for *nos* expression in gills of a paedomorphic amphibian, the Mexican axolotl, which
445 maintains gill structures in adulthood. Taking into account the different evolutionary and
446 developmental origin of internal and external gills [50], the conservation of *nos3*
447 expression in gills indicated that the NO signaling system could be indeed fundamental for
448 the physiology and development of this structure in the axolotl, and perhaps generally in
449 pre-metamorphic amphibians. Therefore, our data highlighted that the expression of at
450 least one *nos* gene has a functional role in gnathostome gills.
451 Recently, a single origin of pharyngeal gills predating the divergence of cyclostomes and
452 gnathostomes was suggested [36]. Therefore, we investigated whether either of the two
453 arctic lamprey *nos* paralogs is expressed in developing gills, but found them expressed
454 mainly in the nervous system, mouth and pharynx, similarly to the expression pattern
455 previously reported in the cephalochordate amphioxus [51,52]. This led us to speculate
456 that either the expression of *nos* genes in gills was acquired in gnathostomes after the
457 divergence from cyclostomes, or alternatively, gill expression was a feature of their last
458 common ancestor but lost in the lineage of cyclostomes.
459 In conclusion, our findings pave the way for future studies that aim to investigate the
460 ontogenetic role of nitric oxide in gill development of aquatic vertebrates. It would be
461 interesting to understand more about species-specific regulatory mechanisms that drive
462 different *nos* genes expression patterns in gills in different species.
463
464
465

Methods

Phylogenetic analysis

Nos sequences used for evolutionary analyses were retrieved from NCBI, Ensembl, Skatebase and DDBJ databases (electronic supplementary material, Table 1). We used proteins from *Homo sapiens*, *Anolis carolinensis* and *Xenopus tropicalis* as internal references, and two non-vertebrate chordates as outgroups: the cephalochordate *Branchiostoma lanceolatum* NosA, NosB and NosC, and the tunicate *Ciona robusta* Nos.

Nos sequences from bowfin (*A. calva*) were obtained from a draft genome assembly [23]. Lamprey *nosA* and *nosB* genes were obtained by TBLASTN v2.2.31+ searches [53] from the v1.0 draft genome of arctic lamprey *L. camtschaticum* [25] and the germ line draft genome of sea lamprey *P. marinus* [54]. Initial predictions were extended, corrected, and confirmed by RACE PCRs in the case of *L. camtschaticum*. Both *P. marinus nosA* and *nosB* were manually curated using Wise2 [55]. The single *nos* gene sequence from the inshore hagfish *E. burgeri* was obtained from a *de novo* transcriptome assembly [56]. Sequences of *nos1*, *nos2,* and *nos3* genes from the cloudy catshark *S. torazame* were obtained from a *de novo* transcriptome assembly [56]. A partial *nos1* sequence (g15096.t1) was found in the European eel *A. anguilla* transcriptome database (EeelBase 2.0) but it was deliberately excluded because of alignment ambiguities.

For phylogenetic analysis, Nos amino acid sequences were aligned using the MUSCLE algorithm [57] as implemented in MEGAX (v10.2.4) [58]. The alignment was trimmed by trimAl v1.2rev59 [59] and then formatted into a nexus file using readAl (bundled with the trimAl package) (electronic supplementary material, File S1). The Bayesian inference tree was constructed using MrBayes v3.2.6 [60], under the assumption of an LG+I+G evolutionary model. Two independent MrBayes runs of 2,000,000 generations were performed, with four chains each and a temperature parameter value of 0.05. The tree was

considered to have reached convergence when the standard deviation stabilized under a value of <0.01. A burn-in of 25% of the trees was performed to generate the consensus tree (1,500,000 post-burnt-in trees). The maximum-likelihood (ML) phylogenetic tree was inferred on the same multi sequence alignment (electronic supplementary material, file S1) using IQ-TREE version 2.1.3 (Nguyen et al., 2015) with 1000 replicates, using automatic selection of best-fit model with ModelFinder (Kalyaanamoorthy et al., 2017) and branch support assessed with the ultrafast bootstrap approximation (Hoang et al., 2018) (electronic supplementary material, figure S2).

Commented [SD2]: D.T. Hoang, O. Chernomor, A. von Haeseler, B.Q. Minh, and L.S. Vinh (2018) UFBoot2: Improving the ultrafast bootstrap approximation. Mol. Biol. Evol., 35:518–522. https://doi.org/10.1093/molbev/msx281

S. Kalyaanamoorthy, B.Q. Minh, T.K.F. Wong, A. von Haeseler, and L.S. Jermiin (2017) ModelFinder: fast model selection for accurate phylogenetic estimates. Nat. Methods, 14:587–589. DOI: 10.1038/nmeth.4285

L.-T. Nguyen, H.A. Schmidt, A. von Haeseler, and B.Q. Minh (2015) IQ-TREE: A fast and effective stochastic algorithm for estimating maximum likelihood phylogenies. Mol. Biol. Evol., 32:268-274. https://doi.org/10.1093/molbev/msu300

Selection Analysis

We assessed signals of selection footprints in the *nos* genes by estimating the non-synonymous to synonymous substitution rate ratio (ω = dN/dS). For this, we inferred a phylogenetic tree including the available sequences from vertebrate species clade (as previously described; electronic supplementary material, Table S1 and File S1). Under the assumption of neutral evolution, ω is expected to have a value of 1. Positive and purifying (negative) selection are indicated when ω > 1 and ω < 1, respectively (Nei & Gojobori, 1986). We used the PAML wrapper EasyCodeML 1.31 (Gao et al. 2019) using the codon-aware filtered gene alignments to fit substitution models to the data for ω estimation. We used a two-ratio branch model assuming that specific branches have an ω that differs from that throughout the rest of the tree (Yang, 1998; Yang & Nielsen, 1998, 2002). We did 3 different analyses and in each analysis we tested if all the branches of each clade (nos1, nos 2, nos 3) had a different ω from that throughout the rest of the tree. Pairwise comparisons of these models were performed using likelihood-ratio tests (Anisimova et al., 2001). If the p-value of the LRTs (likelihood-ratio tests) was significant, then we accepted that the value of ω is different in our clade (gene) with respect to the rest of the tree

against to the assumption of an equal ω for all the tree (for all the three genes).

Synteny

With the aim of finding synteny blocks flanking the *nos2* and *nos3* orthologs, we employed the Synteny Database [61,62]. Additional information was retrieved in NCBI, Ensemble (v.102) and Genomicus (v100.01) [61].

Gene expression analysis by *in situ* hybridization

Whole-mount *in situ* hybridization experiments were performed for all *nos* paralogues following species-specific protocols previously described: spotted gar [63], bichir and sturgeon [64], lamprey [65], and shark [66]. Embryos and tissues collection are reported in electronic supplementary material. For spotted gar embryos at 7 dpf (Long & Ballard stage 24) and 11 dpf (Long & Ballard stage 28), longer proteinase K (10 µg/mL) digestion times were performed, respectively 25 and 35 minutes at 24°C. Moreover, endogenous melanin pigment was removed using bleaching solution [(3% hydrogen peroxide (H_2O_2) and 1% potassium hydroxide (KOH) in distillate water (ddH_2O)] for a few minutes. For 14 dpf gar embryos (Long & Ballard stage 31), we performed *in situ* hybridizations on cryosections, as previously described [67], including modifications reported in [68].

Transversal vibratome sections of bichir and sturgeon embryos (thickness 50 µm) were made on whole-mount hybridized embryos upon embedding in gelatin/albumin/glutaraldehyde [50]. Shark embryos were embedded in paraffin after whole-mount *in situ* hybridization assays, and frontal sections (10 µm) were obtained with a microtome.

Real-time PCR

Expression levels of *nos* genes in axolotl *A. mexicanum* gills were analysed by RT-qPCR using specific primers reported in electronic supplementary material, Table S3. The *atpf51* gene was used as a reference and data were analysed using the ΔΔCT method.

Data accessibility

Accession numbers of protein sequences used in the phylogenetic analysis are available in electronic supplementary material, Table S1. Primer sequences used for the synthesis of *in situ* hybridization riboprobes and in quantitative real-time PCR experiments are given in electronic supplementary material, Table S3.

Authors' contributions

Conceptualization: GA, JHP, SDA. Investigation, data curation and formal analyses: GA, JPA, DO, JS, IS, VS, RV, JHP. Writing-original draft: GA, SDA. Writing-review and editing: all authors. Supervision: SDA. All authors gave final approval for publication.

Competing interests

The authors declare no competing interests.

Funding

Giovanni Annona was supported by the Research grant POR Campania FSE 2014/2020 (IT) and by the EMBO Short Term Fellowship (# 6936) to visit the Postlethwait laboratory in Oregon (USA) and for the field trip in Louisiana (USA). Jan Stundl is supported by the European Union's Horizon 2020 research and innovation program under the Marie Skłodowska-Curie grant agreement No. 897949. Vladimir Soukup is supported by the Charles University Research Centre program No. 204069 and grant SVV260571/2020.

Randal Voss and the Ambystoma Genetic Stock Center are supported by the National Institutes of Health, USA (P40OD019794). John H. Postlethwait is supported by the R01 OD011116 grant from the US National Institutes of Health. Salvatore D'Aniello is supported by the NOEVO grant from the SZN.

Acknowledgments

The authors thank Allyse Ferrara and Quenton Fontenot, Louisiana State University (USA), for their help in the generation of spotted gar embryos, Fumiaki Sugahara for his help in the interpretation of results in the arctic lamprey, Anna Pospisilova for technical assistance with bichir and sturgeon *in situ* hybridizations, and Martin Psenicka, Roman Franek, Michaela Fucikova, Marek Rodina, David Gela, Martin Kahanec for sterlet sturgeon spawns. A special thanks to Robert Cerny for the establishment of the African bichirs colony at the Charles University in Prague, and to Jordi Paps for his help on maximum-likelihood phylogenetic inference. We are indebted also to Silvia Perea and Iker Irisarri for their help in the selection analyses.

References

1. Koshland D. The molecule of the year. Science (80-). 1992;258: 1861–1861.
2. Strijdom H, Chamane N, Lochner A. Nitric oxide in the cardiovascular system: a simple molecule with complex actions. Cardiovasc J Afr. 2009;20: 303–10.
3. Esplugues J V. NO as a signalling molecule in the nervous system. Br J Pharmacol. 2002;135: 1079–1095.
4. Bogdan C. Nitric oxide and the immune response. Nat Immunol. 2001;2: 907–916.
5. Knott AB, Bossy-Wetzel E. Nitric Oxide in Health and Disease of the Nervous

System. Antioxid Redox Signal. 2009;11: 541–553.

6. Kamm A, Przychodzen P, Kuban-Jankowska A, Jacewicz D, Dabrowska AM, Nussberger S, et al. Nitric oxide and its derivatives in the cancer battlefield. Nitric Oxide. 2019;93: 102–114.

7. Santolini J. What does ldquo NO-Synthase rdquo stand for ? Front Biosci. 2019;24: 133–171.

8. Andreakis N, D'Aniello S, Albalat R, Patti FP, Garcia-Fernandez J, Procaccini G, et al. Evolution of the Nitric Oxide Synthase Family in Metazoans. Mol Biol Evol. 2011;28: 163–179.

9. Berg DA, Belnoue L, Song H, Simon A. Neurotransmitter-mediated control of neurogenesis in the adult vertebrate brain. Development. 2013;140: 2548–2561.

10. Steinert JR, Chernova T, Forsythe ID. Nitric Oxide Signaling in Brain Function, Dysfunction, and Dementia. Neurosci. 2010;16: 435–452.

11. Moncada S, Higgs EA. The discovery of nitric oxide and its role in vascular biology. Br J Pharmacol. 2006;147: S193–S201.

12. Namba T, Koike H, Murakami K, Aoki M, Makino H, Hashiya N, et al. Angiogenesis Induced by Endothelial Nitric Oxide Synthase Gene Through Vascular Endothelial Growth Factor Expression in a Rat Hindlimb Ischemia Model. Circulation. 2003;108: 2250–2257.

13. Förstermann U, Sessa WC. Nitric oxide synthases: regulation and function. Eur Heart J. 2012;33: 829–837.

14. Postlethwait J, Amores A, Force A, Yan YL. The zebrafish genome. Methods Cell Biol. 1998;60: 149–163.

15. Amores A. Zebrafish hox Clusters and Vertebrate Genome Evolution. Science (80-). 1998;282: 1711–1714.

16. Taylor JS, Van de Peer Y, Braasch I, Meyer A. Comparative genomics provides evidence for an ancient genome duplication event in fish. Schilling T, Wilson S, editors. Philos Trans R Soc London Ser B Biol Sci. 2001;356: 1661–1679.
17. Jaillon O, Aury J-M, Brunet F, Petit J-L, Stange-Thomann N, Mauceli E, et al. Genome duplication in the teleost fish Tetraodon nigroviridis reveals the early vertebrate proto-karyotype. Nature. 2004;431: 946–957.
18. Tota B, Amelio D, Pellegrino D, Ip YK, Cerra MC. NO modulation of myocardial performance in fish hearts. Comp Biochem Physiol Part A Mol Integr Physiol. 2005;142: 164–177.
19. Agnisola C, Pellegrino D. Role of nitric oxide in vascular regulation in fish. Advances in Experimental Biology. 2007. pp. 293–310.
20. Donald JA, Forgan LG, Cameron MS. The evolution of nitric oxide signalling in vertebrate blood vessels. J Comp Physiol B. 2015;185: 153–171.
21. Hughes LC, Ortí G, Huang Y, Sun Y, Baldwin CC, Thompson AW, et al. Comprehensive phylogeny of ray-finned fishes (Actinopterygii) based on transcriptomic and genomic data. Proc Natl Acad Sci. 2018;115: 6249–6254.
22. Du K, Stöck M, Kneitz S, Klopp C, Woltering JM, Adolfi MC, et al. The sterlet sturgeon genome sequence and the mechanisms of segmental rediploidization. Nat Ecol Evol. 2020;4: 841–852.
23. Thompson A, Hawkins M, Parey E, Wcisel D, Ota T, Kawasaki K, et al. The genome of the bowfin (Amia calva) illuminates the developmental evolution of ray-finned fishes. Nat Res. 2020.
24. Gallant JR, Losilla M, Tomlinson C, Warren WC. The genome and adult somatic transcriptome of the mormyrid electric fish paramormyrops kingsleyae. Genome Biol Evol. 2017;9: 3525–3530.

641 25. Mehta TK, Ravi V, Yamasaki S, Lee AP, Lian MM, Tay B-H, et al. Evidence for at
642 least six Hox clusters in the Japanese lamprey (Lethenteron japonicum). Proc Natl
643 Acad Sci. 2013;110: 16044–16049.
644 26. Xu P, Xu J, Liu G, Chen L, Zhou Z, Peng W, et al. The allotetraploid origin and
645 asymmetrical genome evolution of the common carp Cyprinus carpio. Nat Commun.
646 2019;10: 4625.
647 27. Berthelot C, Brunet F, Chalopin D, Juanchich A, Bernard M, Noël B, et al. The
648 rainbow trout genome provides novel insights into evolution after whole-genome
649 duplication in vertebrates. Nat Commun. 2014;5: 3657.
650 28. Lien S, Koop BF, Sandve SR, Miller JR, Kent MP, Nome T, et al. The Atlantic
651 salmon genome provides insights into rediploidization. Nature. 2016;533: 200–205.
652 29. Braasch I, Gehrke AR, Smith JJ, Kawasaki K, Manousaki T, Pasquier J, et al. The
653 spotted gar genome illuminates vertebrate evolution and facilitates human-teleost
654 comparisons. Nat Genet. 2016;48: 427–437.
655 30. Gibbins IL, Olsson C, Holmgren S. Distribution of neurons reactive for NADPH-
656 diaphorase in the branchial nerves of a teleost fish, Gadus morhua. Neurosci Lett.
657 1995;193: 113–116.
658 31. Mauceri A, Fasulo S, Ainis L, Licata A, Rita lauriano E, Martfnez A, et al. Neuronal
659 nitric oxide synthase (nNOS) expression in the epithelial neuroendocrine cell system
660 and nerve fibers in the gill of the catfish, Heteropneustes fossilis. Acta Histochem.
661 1999;101: 437–448.
662 32. Fritsche R, Schwerte T, Pelster B. Nitric oxide and vascular reactivity in developing
663 zebrafish, Danio rerio. Am J Physiol Integr Comp Physiol. 2000;279: R2200–R2207.
664 33. Evans DH. Cell signaling and ion transport across the fish gill epithelium. J Exp Zool.
665 2002;293: 336–347.

34. Haraldsen L, Söderström-Lauritzsen V, Nilsson GE. Oxytocin stimulates cerebral blood flow in rainbow trout (Oncorhynchus mykiss) through a nitric oxide dependent mechanism. Brain Res. 2002;929: 10–14.
35. Pellegrino D, Sprovieri E, Mazza R, Randall D., Tota B. Nitric oxide-cGMP-mediated vasoconstriction and effects of acetylcholine in the branchial circulation of the eel. Comp Biochem Physiol Part A Mol Integr Physiol. 2002;132: 447–457.
36. Gillis JA, Tidswell ORA. The Origin of Vertebrate Gills. Curr Biol. 2017;27: 729–732.
37. Warga RM, Nüsslein-Volhard C. Origin and development of the zebrafish endoderm. Development. 1999;126: 827–38.
38. Poon K-L, Richardson M, Korzh V. Expression of zebrafishnos2b surrounds oral cavity. Dev Dyn. 2008;237: 1662–1667.
39. Lepiller S, Franche N, Solary E, Chluba J, Laurens V. Comparative analysis of zebrafish nos2a and nos2b genes. Gene. 2009;445: 58–65.
40. Lind M, Hayes A, Caprnda M, Petrovic D, Rodrigo L, Kruzliak P, et al. Inducible nitric oxide synthase: Good or bad? Biomed Pharmacother. 2017;93: 370–375.
41. Dehal P, Boore JL. Two Rounds of Whole Genome Duplication in the Ancestral Vertebrate. Holland P, editor. PLoS Biol. 2005;3: e314.
42. Tota B, Amelio D, Cerra MC, Garofalo F. The morphological and functional significance of the NOS/NO system in the respiratory, osmoregulatory, and contractile organs of the African lungfish. Acta Histochem. 2018;120: 654–666.
43. Tipsmark CK. Regulation of Na+/K+-ATPase activity by nitric oxide in the kidney and gill of the brown trout (Salmo trutta). J Exp Biol. 2003;206: 1503–1510.
44. Ebbesson LOE. Nitric oxide synthase in the gill of Atlantic salmon: colocalization with and inhibition of Na+,K+-ATPase. J Exp Biol. 2005;208: 1011–1017.
45. Hyndman KA, Choe KP, Havird JC, Rose RE, Piermarini PM, Evans DH. Neuronal

691 nitric oxide synthase in the gill of the killifish, Fundulus heteroclitus. Comp Biochem
692 Physiol Part B Biochem Mol Biol. 2006;144: 510–519.
693 46. Campos-Perez JJ, Ward M, Grabowski PS, Ellis AE, Secombes CJ. The gills are an
694 important site of iNOS expression in rainbow trout Oncorhynchus mykiss after
695 challenge with the Gram-positive pathogen Renibacterium salmoninarum.
696 Immunology. 2000;99: 153–161.
697 47. Mistri A, Kumari U, Mittal S, Mittal AK. Immunohistochemical localization of nitric
698 oxide synthase (NOS) isoforms in epidermis and gill epithelium of an angler catfish,
699 Chaca chaca (Siluriformes, Chacidae). Tissue Cell. 2018;55: 25–30.
700 48. Force A, Lynch M, Pickett FB, Amores A, Yan YL, Postlethwait J. Preservation of
701 duplicate genes by complementary, degenerative mutations. Genetics. 1999;151:
702 1531–45.
703 49. Farnsworth DR, Saunders LM, Miller AC. A single-cell transcriptome atlas for
704 zebrafish development. Dev Biol. 2020;459: 100–108.
705 50. Stundl J, Pospisilova A, Jandzik D, Fabian P, Dobiasova B, Minarik M, et al. Bichir
706 external gills arise via heterochronic shift that accelerates hyoid arch development.
707 Elife. 2019;8: e43531.
708 51. Annona G, Caccavale F, Pascual-Anaya J, Kuratani S, De Luca P, Palumbo A, et al.
709 Nitric Oxide regulates mouth development in amphioxus. Sci Rep. 2017;7: 8432.
710 52. Caccavale F, Annona G, Subirana L, Escriva H, Bertrand S, D'Aniello S. Crosstalk
711 between Nitric Oxide and Retinoic Acid pathways is essential for amphioxus pharynx
712 development. bioRxiv. 2020.
713 53. Altschul S. Gapped BLAST and PSI-BLAST: a new generation of protein database
714 search programs. Nucleic Acids Res. 1997;25: 3389–3402.
715 54. Smith JJ, Timoshevskaya N, Ye C, Holt C, Keinath MC, Parker HJ, et al. The sea

716 lamprey germline genome provides insights into programmed genome
717 rearrangement and vertebrate evolution. Nat Genet. 2018;50: 270–277.
718 55. Madeira F, Park YM, Lee J, Buso N, Gur T, Madhusoodanan N, et al. The EMBL-
719 EBI search and sequence analysis tools APIs in 2019. Nucleic Acids Res. 2019;47:
720 W636–W641.
721 56. Pascual-Anaya J, Sato I, Sugahara F, Higuchi S, Paps J, Ren Y, et al. Hagfish and
722 lamprey Hox genes reveal conservation of temporal colinearity in vertebrates. Nat
723 Ecol Evol. 2018;2: 859–866.
724 57. Edgar RC. MUSCLE: multiple sequence alignment with high accuracy and high
725 throughput. Nucleic Acids Res. 2004;32: 1792–1797.
726 58. Kumar S, Stecher G, Li M, Knyaz C, Tamura K. MEGA X: Molecular Evolutionary
727 Genetics Analysis across Computing Platforms. Battistuzzi FU, editor. Mol Biol Evol.
728 2018;35: 1547–1549.
729 59. Capella-Gutierrez S, Silla-Martinez JM, Gabaldon T. trimAl: a tool for automated
730 alignment trimming in large-scale phylogenetic analyses. Bioinformatics. 2009;25:
731 1972–1973.
732 60. Ronquist F, Teslenko M, van der Mark P, Ayres DL, Darling A, Höhna S, et al.
733 MrBayes 3.2: Efficient Bayesian Phylogenetic Inference and Model Choice Across a
734 Large Model Space. Syst Biol. 2012;61: 539–542.
735 61. Nguyen NTT, Vincens P, Roest Crollius H, Louis A. Genomicus 2018: karyotype
736 evolutionary trees and on-the-fly synteny computing. Nucleic Acids Res. 2018;46:
737 D816–D822.
738 62. Catchen JM, Conery JS, Postlethwait JH. Automated identification of conserved
739 synteny after whole-genome duplication. Genome Res. 2009;19: 1497–1505.
740 63. Jowett T, Yan Y-L. Double fluorescent in situ hybridization to zebrafish embryos.

741 Trends Genet. 1996;12: 387–389.
742 64. Minarik M, Stundl J, Fabian P, Jandzik D, Metscher BD, Psenicka M, et al. Pre-oral
743 gut contributes to facial structures in non-teleost fishes. Nature. 2017;547: 209–212.
744 65. Sugahara F, Murakami Y, Kuratani S. Gene Expression Analysis of Lamprey
745 Embryos. In Situ Hybridization Methods. 2015. pp. 263–278.
746 66. Adachi N, Takechi M, Hirai T, Kuratani S. Development of the head and trunk
747 mesoderm in the dogfish, Scyliorhinus torazame : II. Comparison of gene expression
748 between the head mesoderm and somites with reference to the origin of the
749 vertebrate head. Evol Dev. 2012;14: 257–276.
750 67. Strähle U, Blader P, Adam J, Ingham PW. A simple and efficient procedure for non-
751 isotopic in situ hybridization to sectioned material. Trends Genet. 1994;10: 75–76.
752 68. Jowett T, Ingham PW, Henrique D, Lettice L, Wilkinson D, Yan YL. An EMBO
753 practical course. Univ Newcastle, Newcastle. 1995; 50.
754